Ratelimiting step and substrate accessibility of cellobiohydrolase Cel6A from Trichoderma reesei

Christensen, Stefan Jarl; Kari, Jeppe; Badino, Silke Flindt; Borch, Kim; Westh, Peter

Published in:
F E B S Journal

DOI:
10.1111/febs.14668

Publication date:
2018

Document Version
Peer reviewed version

Citation for published version (APA):
Christensen, S. J., Kari, J., Badino, S. F., Borch, K., & Westh, P. (2018). Ratelimiting step and substrate accessibility of cellobiohydrolase Cel6A from Trichoderma reesei. *F E B S Journal*, *285*(23), 4482-4493. https://doi.org/10.1111/febs.14668

Received Date : 09-May-2018

Revised Date : 11-Sep-2018

Accepted Date : 28-Sep-2018

Rate-limiting step and substrate accessibility of cellobiohydrolase Cel6A from *Trichoderma reesei*

Stefan Jarl Christensen[1], Jeppe Kari[1], Silke Flindt Badino[1], Kim Borch[2] and Peter Westh[1*]

1. Research Unit for Functional Biomaterials, Department of Science and Environment, Roskilde University. 1 Universitetsvej, Build. 28.C, DK-4000, Roskilde, Denmark. Email: sjarlc@ruc.dk, sbadino@ruc.dk, jkari@ruc.dk, pwesth@ruc.dk
2. Novozymes A/S, Krogshøjvej 36, DK-2880, Bagsværd, Denmark. E-mail: kimb@novozymes.com

*__Corresponding author__: Email: pwesth@ruc.dk ; Telephone: +45 4674 2879; Fax: +45 4674 3011

Running title: Rate-limiting step and substrate accessibility of *Tr*Cel6A

Article type : Original Articles

Article type: Original article

Abbreviations: CBH, Cellobiohydrolase; GH, Glycoside hydrolase; HPAEC-PAD, High-Performance Anion-Exchange Chromatography with Pulsed Amperometric Detection; MM, Michaelis Menten; *n,* processivity number; n^{prod}, processivity number based on product concentrations; n^{theo}, theoretical processivity number; RAC, regenerated amorphous cellulose.

Enzymes: *Tr*Cel6A, non-reducing end acting Cellobiohydrolase (**EC 3.2.1.91**) from *Trichoderma reesei;* TrCel7A, reducing end acting Cellobiohydrolase (**EC 3.2.1.176**) from *Trichoderma reesei*

Key words: Cellobiohydrolases, Cel6A, Quenched-flow, Enzyme kinetics, Cellulose

This article has been accepted for publication and undergone full peer review but has not been through the copyediting, typesetting, pagination and proofreading process, which may lead to differences between this version and the Version of Record. Please cite this article as doi: 10.1111/febs.14668

Conflict of interest: Kim Borch works for Novozymes A/S, a major manufacturer of industrial enzymes.

Abstract

The Cellobiohydrolase Cel6A is an important component of enzyme cocktails for industrial degradation of lignocellulosic biomass. However, the kinetics of this enzyme acting on its natural, insoluble substrate remains sparsely investigated. Here, we studied Cel6A from *Trichoderma reesei* with respect to adsorption, processivity and kinetics both in the steady state and pre-steady state regimes, on microcrystalline and amorphous cellulose. We found that slow dissociation (k_{off}) was limiting the overall reaction rate, and we suggest that this leads to an accumulation of catalytically inactive complexes in front of obstacles and irregularities on the cellulose surface. The processivity number of Cel6A was low on both investigated substrates (5-10), and this suggested a rugged surface with short obstacle-free path-lengths. The turnover of the inner catalytic cycle (the reactions of catalysis in one processive step) was too fast to be fully resolved, but a minimum value of about 20 s^{-1} could be established. This is among the highest values reported hitherto for a cellulase, and it underscores the catalytic efficiency of Cel6A. Conversely, we found that Cel6A had a poor ability to recognize attack sites on the cellulose surface. On amorphous cellulose, for example, Cel6A was only able to initiate hydrolysis on about 4% of the sites to which it could adsorb. This probably reflects high requirements of Cel6A to the architecture of the site. We conclude that compared to the other cellobiohydrolase, Cel7A, secreted by *T. reesei*, Cel6A is catalytically more efficient but less capable of attacking a broad range of structurally distinct sites on the cellulose surface.

Introduction

Cellobiohydrolases (CBHs) are processive glycoside hydrolases (GHs) that catalyze the hydrolysis of cellulose [1]. The fungal CBHs are members of GH family 6 and 7 and are denoted Cel6 and Cel7, respectively. Cel7A and Cel6A are the most abundantly produced and secreted cellulases in the model fungus *Trichoderma reesei* and major components of industrial enzyme cocktails [2, 3]. The two enzymes share some functional similarities, as they both catalyze hydrolysis of cellulose and generate cellobiose as the main product. However, they differ with respect to e.g. overall protein fold, direction of processive motion and hydrolytic cleavage mechanism [4-6]. Cel7A is by far the most extensively characterized cellulase regarding hydrolytic mechanism, structure and kinetics (reviewed in [7]), while only a few studies has described the kinetics of Cel6A [8-12]. Here, we report a detailed kinetic study on *T. reesei* Cel6A (*Tr*Cel6A) with emphasis on the rate-limiting step and the enzyme's ability to access the substrate (*i.e.* initiate hydrolysis on the heterogeneous surface of the insoluble substrate).

Cel6A attacks the non-reducing end of a cellulose strand, and acts in a processive manner, meaning that it remains associated with the strand while sequentially generating new soluble products. Each hydrolytic cleavage is carried out by an inverting mechanism [1, 6, 13]. This process is a complex,

multistep reaction, and current structural and kinetic insights are insufficient to support extensive modeling of all putative steps. Instead, some understanding may be gained by analyzing kinetic data with respect to a simplified description with three composite reaction steps: adsorption, inner catalytic cycle (hydrolysis and processive movement), and dissociation [14]. In the present study, we applied this kinetic approach to experimental data in both the steady-state and pre-steady-state regimes, and to two different types of cellulosic substrates, microcrystalline Avicel, and regenerated amorphous cellulose (RAC). We found, that the maximal steady state rate of Cel6A was governed by slow dissociation (the composite rate constant, k_{off}, was rate limiting) and that the enzyme follows the so-called obstacle theory for processive enzymes [15]. Additionally, we demonstrated that the difference in hydrolytic activity on crystalline and amorphous cellulose lies primarily in the differences in substrate accessibility, most likely resulting from dissimilar substrate morphologies while the underlying rate constants are of comparable size. Finally, our results were compared to published data for Cel7A from *T. reesei* (TrCel7A), showing that the two enzymes were kinetically quite different. Hence, Cel6A is an order of magnitude faster than Cel7A both with respect to the chemical reactions of the inner catalytic cycle and the adsorption/desorption dynamics. Conversely, Cel6A is much less efficient than Cel7A in finding attack sites on the heterogenous cellulose surface.

Results and data analysis

Quenched-flow measurements

Samples with very short reaction times (down to 0.25 s) were prepared in a recently developed quenched-flow instrument [16], and their content of soluble sugars was quantified by High-Performance Anion-Exchange Chromatography with Pulsed Amperometric Detection (HPAEC-PAD) analyses of the supernatants. Results of these measurements on Avicel and RAC showing the sum of the cellobiose and cellotriose concentrations as a function of reaction time are given in Fig. 1.

It appeared that the Cel6A reaction started quickly, and none of the quenched-flow experiments provided a full resolution of the pre-steady state kinetics. However, it could be partially resolved as steady state was not established until about 1 s into the experiment (as indicated by a linear progress curve). To analyze the results in Fig. 1 further we performed a non-linear regression analysis with respect to a rate equation derived from a simplified reaction scheme for processive cellulases, which we have earlier applied in characterization of TrCel7A [14].

The reaction in Scheme 1 introduces three composite rate constants k_{on} (adsorption and formation of enzyme-substrate complex), k_{hyd} (hydrolytic reaction and processive movement) and k_{off} (dissociation). A fourth parameter in the model, *n*, signified the processivity number; *i.e*. the average number of hydrolytic reactions performed on one strand without dissociation. The subscripts in C_m, C_{m-1}, C_{m-2} etc. denotes the polymeric state of the substrate (e.g. how many cellobiose moieties has been removed by the enzyme). For further detail see Praestgaard, *et al.* [14].
The regression analyses showed that the parameters k_{on}, k_{off} and *n* could be determined with reasonable precision and their values are listed in Table 1. The last parameter, k_{hyd}, varied uncontrollably in the regressions and could not be determined from these experiments; probably due to lack of data points at very low reaction times (before the inflection points of the red curves in Fig. 1). It would require still higher experimental time resolution to find k_{hyd} with reasonable

precision, but the other parameters were well determined. We found that when k_{hyd} was fixed to values below ~*75* s^{-1} the model fitted the experimental data poorly, resulting in a large increase in the residual sum of square and a systematic change in the three other parameters that vary to compensate for the poor fit. Above this value k_{hyd} neither influenced the overall fit nor the derived parameters significantly. The extent of the burst saturates under conditions where $k_{on}S_0 >> k_{off}$ [14]. Using the substrate loads from the quenched-flow measurements and the rate constants in Table 1, we see that $k_{on}S_0$ is 5-10 fold higher than k_{off} in the current experiments. As shown in Fig. 1, this is enough to obtain a clear burst.

Steady state kinetics

To elucidate the Cel6A reaction further, we studied steady state kinetics by two separate approaches [17, 18] on both Avicel and RAC. Both approaches rely on initial rates, which were approximated from 1 h end-point measurements in this work. The first approach follows conventional Michaelis Menten (MM) theory and hence relies on experiments, where the substrate is in large excess. In practice, this implies separate measurements of the initial rate for a fixed, very low enzyme concentration (low E_0) and a wide range of different substrate loads (S_0). Initial rates for Cel6A acting on Avicel (Fig. 2A) or RAC (Fig. 2B) were plotted as a function of the substrate load and analyzed with respect to Eqn (1), which we henceforth call the conventional MM-equation:

$$^{conv}v = \frac{^{conv}V_{\max} S_0}{^{conv}K_M + S_0} \qquad (1)$$

In Eqn (1), the parameters have their usual meaning, but we note that S_0 and $^{conv}K_M$ are in units of g/L, and not in molar units as in homogenous enzymology. The applicability of Eqn (1) to processive enzymes, and the definition of $^{conv}V_{max}$ and $^{conv}K_M$ with respect to Scheme 1 have been discussed elsewhere [17]. These definitions, however, are not important for the current (comparative) use, and the maximal rate and Michaelis constant in Eqn (1) may be interpreted in the common way. As always, saturation in the conventional MM framework occurs at high substrate loads when essentially all enzyme is associated with substrate. The lines in Fig. 2A and Fig. 2B shows the best fit of Eqn (1) to the experimental data, and the parameters derived from this analysis are listed in Table 2. We note that $^{conv}K_M$ is around an order of magnitude larger than the ratio k_{off}/k_{on} derived from the pre-steady state measurements although in the ideal case, these parameters should be equal [17]. The underlying reasons for this discrepancy cannot be fully elucidated by the current data, but it may rely on differences between experiments with short (quenched flow) and longer (end point measurements) contact times. We also used another, less common steady state approach [18, 19]. This method relies on the idea that the number of non-reducing ends from which the enzyme can initiate hydrolysis (attack sites), on the cellulose surface remains nearly constant in the initial part of the reaction, because new ends become exposed as the enzyme removes cellulose strands from the surface of the particle. Some experimental support of this assumption has been presented elsewhere [18, 19], and if the density of attack site indeed remains nearly constant long enough to perform rate measurements, one can use another type of steady state analysis, which we call the inversed MM-framework [18]. In practice, this approach requires initial rate measurements at a fixed, low substrate load (low S_0) and at gradually increasing enzyme concentrations (E_0). Initial rates

measured under inverse MM conditions were plotted as a function of the enzyme concentration and analyzed with respect to the inversed MM equation [18, 19].

$$^{inv}v = \frac{^{inv}V_{\max} E_0}{^{inv}K_M + E_0} \qquad (2)$$

Eqn (2) introduces a new maximal rate, $^{inv}V_{max}$, which reflects the rate at large excess of enzyme where essentially all attack sites on the substrate surface are occupied (the substrate is saturated with enzyme). The inverse Michaelis constant, $^{inv}K_M$ is the enzyme concentration (in µM) required to reach half of $^{inv}V_{max}$. Kinetic experiments made according to this inverse MM approach are presented in Fig. 2C and Fig. 2D and best fits of Eqn (2) are also shown in these figures. The inverse parameters derived from the analysis are listed in Table 2.

Binding isotherms

We assessed binding of *Tr*Cel6A to Avicel and RAC by measuring the concentration of free enzyme, $E_{free,}$ in equilibrated samples with fixed substrate loads and varying initial enzyme concentrations. The amount of bound enzyme per g substrate (the substrate coverage, Γ) was calculated as $\Gamma = \frac{E_0 - E_{free}}{S_0}$, and plotted against E_{free} as shown in Fig. 2E and F. The data in these figures were fitted to a standard Langmuir isotherm.

$$\Gamma = \Gamma_{\max} \frac{E_{free}}{K_d + E_{free}} \qquad (3)$$

where K_d is the dissociation constant and Γ_{max} is the maximum binding capacity (saturation coverage). Although this approach is overly simplified [20] it accounted reasonably for the data (Fig. 2 E and F) at least within the range of E_{free} covered here. Langmuir parameters are listed in Table 2, and we see that Γ_{max} is ~10 times higher for RAC compared to Avicel.

Product profile

Hydrolysis of the two substrates, Avicel and RAC, by *Tr*Cel6A generated predominantly cellobiose (G2) and cellotriose (G3) as demonstrated in Table 3. The main product was cellobiose, but cellotriose was found in concentrations of ~10-20% of total products. Glucose (G1) was not detectable in Avicel hydrolysis but found in lower concentrations in RAC hydrolysis (~4%). In the current context, we are mostly interested in product profiles because they provide some insight to the processivity number. Several approaches to the estimation of the processivity number from product concentrations (n^{prod}) have been put forward and discussed critically [21], but we will use the ratio ([G2]-[G1])/([G3]+[G1]), which has previously been proposed for an inverting cellulase [22].

Discussion

Rate limiting step

Cel6A is an industrially important, but kinetically poorly characterized enzyme. The nature of rate limitation remains to be investigated, and to address this, we have studied Cel6A from *T. reesei* by a range of methods. We found the steady-state turnover number defined in the usual way, $k_{cat} = {}^{conv}V_{max}/E_0$, was about 0.5 s^{-1} for both insoluble substrates in Table 2. This is in line with values for Cel6A earlier reported by Velleste *et al.* [23]. Gruno *et al.* reported a higher value of around 8 s^{-1} by performing 10 s measurements [24], which is in the same range as the slope/E_0 of the phase subsequent to the burst in Fig. 1 (~2-5 s^{-1}). A much faster specific rate (15-20 s^{-1}) can be derived from the initial slope of the progress curves between 0 and 0.2 s in Fig. 1. This behavior of a rapid initial hydrolysis followed by a slower steady-state rate, as it appears directly from the progress curves in Fig. 1, is analogous to classical burst behavior for soluble enzyme-substrate systems [25, 26]. For soluble systems, this well-known behavior may occur in reactions with two products, if the second product dissociates very slowly from the enzyme. In this case, the pre-steady-state regime will be characterized by a rapid production of the first product, and a concomitant build-up of an intermediate composed of enzyme and the second product [27, 28]. We suggest that the current data for Cel6A represents an analogous mechanism. Thus, if $k_{hyd} >> k_{off}$, Scheme 1 predicts a rapid production of cellobiose in the opening processive sweep before the enzyme encounters the first (slow) dissociation step. There is, however, one fundamental difference between the classical description of the burst phase and the analysis of processive enzymes. To illustrate this difference, we note that very slow dissociation of a processive enzyme (*i.e*. low k_{off} in Scheme 1) would simply imply that the enzyme rarely dissociated and hence progressed forward until the cellulose strand was fully degraded. Rigorous statistic treatment of this phenomenon has shown that the enzyme will continue its processive movement for an average of approximately k_{hyd}/k_{off} steps [29]. This ratio is sometimes called the theoretical- or intrinsic processivitity (n^{theo}). In practice, the theoretical value would be attained if no structural impediments on the cellulose surface affected the processive movement, and in the following, we argue that our results show that such impediments are indeed hampering the movement of Cel6A. Before we discuss evidence for this, however, we notice that this interpretation of the burst phase for Cel6A is analogous to the so-called obstacle theory for rate limitation of the more thoroughly investigated cellulase, Cel7A [14, 15]. To evaluate the influence of structural impediments (or obstacles) we first estimate the theoretical processivity, $n^{theo} \sim k_{hyd}/k_{off}$, for Cel6A on RAC and Avicel. The denominator, k_{off} could be derived from the quenched-flow measurements and was around 0.35 s^{-1} (Table 1), but k_{hyd} was too large to be determined precisely with the available time resolution. As mentioned above, however, we directly measured specific rates up to 20 s^{-1} from the slope of the progress curve (Fig. 1). The degree of enzyme saturation, $\frac{S_0}{S_0 + k_{off}/k_{on}}$, was about 0.8 in these measurements and it follows that the minimal value of k_{hyd} is about 20-25 s^{-1}. This is among the highest turnover reported for cellulases acting on insoluble substrate. Still higher turnover rates (about 100 s^{-1}) of β-1,4 glycosidic bonds have been reported for chitinases acting on crystalline chitin [30, 31], which is a related recalcitrant substrate. This suggests that the relatively low specific activity (typically <1 s^{-1}) observed for cellulolytic enzymes under normal experimental conditions is not associated with slow conversion of the β-1,4 bond, but must rely on other slow steps including non-covalent changes. It is also interesting to note that the

minimum value for k_{hyd} found here is slightly faster than k_{cat} for the conversion of soluble cellooligosaccharides by Cel6A [8, 32]. This faster conversion of a solid substrate may appear counterintuitive in light of the intermolecular interactions in the cellulose particle. On a practical level, this suggests that turnover of a soluble substrate cannot be used as an upper limit of catalytic efficacy for Cel6A and one possible explanation could be the formation of non-productive complexes with oligosaccharides. The comparably high value of k_{hyd} obviously supports earlier suggestions that Cel6A is catalytically efficient [12], but it also illustrates that the theoretical processivity of this enzyme is much higher ($k_{hyd}/k_{off} \geq 20\ s^{-1}/0.35\ s^{-1} \sim 60$) than the experimental processivity number around 5-12, which was consistently found in modeling of the pre-steady-state data (Table 1), product profiles (Table 3) and in an earlier work [22]. The observation that the theoretical processivity much exceeds experimental values ($n << n^{theo}$) suggests that slow dissociation of Cel6A trapped in front of a steric obstacles on the cellulose surface (see Fig. 3) governs the maximal rate at steady state. This also explains the early burst seen in Fig. 1 because a fast production of n cellobiose molecules per enzyme precedes the build-up of trapped Cel6A. These results also suggest that only a low fraction of enzymes is active at steady state (fig. 2A+B). In fact, from our estimate of k_{hyd} (~20 s^{-1}) we can say that the active population is well below 10% under high substrate loads. We conclude that slow dissociation governs the maximal rate of Cel6A at least for the substrates studied here. Earlier work using a highly crystalline substrate has found higher experimental processivities of Cel6A [10], and this may reflect a smoother surface with less obstacles. In this case, other factors may be equally or more important for rate limitation.

Substrate accessibility

To illustrate what we mean by substrate accessibility, we first note that Cel6A must adsorb to a site on the substrate surface and in a second step combine with a non-reducing end of a cellulose strand to form a catalytically competent enzyme-substrate complex. We will categorize surface sites based on these two steps and use the term “adsorption site” for any locus where Cel6A can bind. Some adsorption sites will have a local structure (including an available non-reducing end) that allows the formation of a catalytically competent enzyme complex, and we will call these “attack sites”. The enzyme cannot form a complex without adsorbing, and it follows that the number of adsorption sites will be equal to or larger than the number of attack sites. Experimentally, the number of adsorption sites can be readily assessed from binding isotherms. Although the binding of cellulases is complex and involves dissimilar sites [20] it is often practical to approximate their adsorption by a simple Langmuir isotherm. In this case, the maximal coverage, Γ_{max}, provides an operational measure of the density of adsorption sites. Attack sites are more challenging to quantify experimentally, but some recent work has addressed this problem [18, 33] and devised workable approaches where the number of attack sites is estimated from kinetic measurements. One approach is to use the ratio of kinetic parameters from conventional- and inverse MM analysis. Thus, if Γ_{attack} denotes the density of attack sites in units of mol g^{-1} cellulose, we may write [18]

$$\Gamma_{attack} = \frac{^{inv}V_{max} / S_0}{^{conv}V_{max} / E_0} \qquad (4)$$

To illustrate the intuitive meaning of Eqn (4), we note that the numerator is the rate of product formation, when all attack sites are occupied (in units of μmol $s^{-1}g^{-1}$ cellulose, see Table 2). The denominator reflects how quickly each attack sites is turned over (in s^{-1}), and it follows that the ratio in Eqn (4) is the density of attack sites in μmol/g. We stress that Eqn (4) gives a rough estimate of the attack-site density but it has been found useful for comparative purposes, which is also the aim of the current discussion. First, we notice that RAC (Γ_{max} = 3.6 μmol/g) has an order of magnitude more adsorption sites per unit mass compared to Avicel (Γ_{max} = 0.37 μmol/g). This probably reflects that differences in packing and morphology leads to a larger specific surface area of RAC. More importantly, we found that the density of attack sites for Cel6A, Γ_{attack}, (Table 2) was much lower than the density of adsorption sites (Γ_{max}). Specifically, attack sites accounted for 16 % of the adsorption sites for Avicel and only 4% for RAC. This shows that Cel6A is a selective enzyme that can only attack a small fraction of the sites to which it adsorbs. We have previous referred to this as a high physical specificity [12]. Thus, the normal definition of high specificity implies that an enzyme is only capable to catalyze a narrow range of chemical reactions and/or attack one or a few highly related types of substrates. In other words, this is a chemical specificity. In the current systems, the "right" chemical bond (the β-1,4 glycosidic bond) is abundant, but Cel6A is only able to attack a small subset of the sites to which it can bind. It follows that Cel6A is selective with respect to the physical properties (i.e. the structure) of the substrate surface. Further inspection of Table 2 shows that the total number of attack sites is about two-fold higher for RAC compared to Avicel, and we conclude that although RAC is a much more accessible substrate (ten-fold higher Γ_{max}) it is only moderately more reactive because Cel6A cannot attack most of the additionally exposed sites.

One particularly interesting aspect of Γ_{attack} is that it can convert the mass load of substrate into an apparent molar concentration of attack sites, $C_{attack} = \Gamma_{attack} S_0$. Using this approach, we first see that C_{attack} was quite low in the quenched flow measurements in Fig. 1, where S_0 was respectively 8.0 g/L and 1.8 g/L for Avicel and RAC (C_{attack} ~ 0.2-0.5 μM). This is comparable with the enzyme concentration (0.2 μM) is these experiments, and implies that the processivity cannot be read directly from the extent of the burst as in cases with large excess of substrate [14]. Instead, the processivity can be estimated from these measurements through regression analysis as described above and reported in Table 1. Another aspect of C_{attack} is that it elucidates the long-standing problem of directly comparing the kinetics of cellulases acting on different substrates. This problem is particular to insoluble substrates and occurs because it is generally not possible to establish whether measured changes in enzyme activity rely on differences in rate constants or substrate accessibility. By quantifying the latter, we could at least in principle compare rate constants for Cel6A on different substrates. For the current data, comparisons of k_{on} appears particularly relevant. Results in Table 1 showed that this second order rate constant was larger on RAC (0.93 $(g/l)^{-1}s^{-1}$) compared to Avicel (0.29 $(g/l)^{-1}s^{-1}$). We converted these mass-based parameters into conventional molar unit rate constants ($^{molar}k_{on}$) by defining the k_{on} determined in Fig. 1 as $k_{on} = {}^{molar}k_{on}\,\Gamma_{attack}$. By dividing k_{on} with Γ_{attack} we estimate $^{molar}k_{on}$ to be respectively 7 $\mu M^{-1}s^{-1}$ (RAC) and 5 $\mu M^{-1}s^{-1}$ (Avicel). This shows that the (molar) rate constant that governs complex formation is quite similar for the two substrates, and hence that the faster association with RAC as indicated in Table 1 primarily reflects that this substrate has more attack sites, which is summarized in the conceptional illustration in Fig. 3. The molar rate constants also serve to show that in spite of its complicated structure, the Cel6A-cellulose complex forms very rapidly. Thus, for enzyme concentrations of few μM (which are

frequently used in experimental work) the half time for complex formation is only tens of ms; indeed, fast considering that the highest steady-state turnover, k_{cat}, is about 0.5 s^{-1}.

Comparison of Cel6A and Cel7A

One key result in this work was that k_{off} for Cel6A was quite low. This gave rise to a typical burst behavior and it meant that that dissociation was the limiting step for the maximal rate at steady state (Fig. 3). This behavior is analogous to several earlier reports on the other cellobiohydrolase, Cel7A, secreted by *T. reesei*. This similarity hints that dissociation plays a dominant role for rate limitation in processive CBHs in general. We argue that slow dissociation could be inherent to processive cellulases because strong interaction with the substrate is necessary to remain associated during processive hydrolysis, and strong binding is inevitably associated to slow dissociation. Comparisons of other results in the current work and literature data for Cel7A points towards distinctive kinetic differences between the two enzymes. One prominent example is the on-off dynamics. Thus, k_{on} and k_{off} values for Cel6A listed in in Table 1 are consistently 20-50 times larger than analogous parameters previously found for Cel7A using similar methods [34, 35]. Interestingly, the net affinity expressed for example as $^{conv}K_M$ is quite similar for the two enzymes [12], and this implies that while the ratio k_{on}/k_{off} is similar, the underlying unidirectional rates are over an order of magnitude faster for Cel6A. This more dynamic nature of the association/dissociation equilibrium for Cel6A is interesting in light of the poor ability of this enzyme to find attack sites (only 4 % of the adsorption sites on RAC could form a catalytically competent complex). This obviously means that Cel6A will experience many unproductive binding/release events before catalysis commences, but this may not be a major disadvantage as these adsorption events are short lived. This behavior is much in contrast to Cel7A, which has much lower on/off dynamics, but the ability to combine productively with essentially all adsorption sites; *i.e.* $\Gamma_{max} \sim \Gamma_{attack}$ for Cel7A [12, 18]. This difference in on/off dynamics is also seen directly from pre-steady state data. Hence, while results from the two enzymes are qualitatively similar with a conspicuous burst phase, the time required to reach steady state is 5-30 s for Cel7A [16, 34, 35] but only about 1 s for Cel6A (Fig. 1). We suggest that these pronounced differences in on/off dynamics for Cel6A and Cel7A can be related to the more accessible substrate binding region in Cel6A. This enzyme has fewer, shorter and more flexible loops to cover the substrate, and the binding region is shorter with fewer pyranose binding sub-sites [5, 6, 36, 37]. It appears reasonable that these structural characteristics could promote rapid association and dissociation of Cel6A.

In conclusion, we found that Cel6A shows burst kinetics and that dissociation is rate is limiting for the maximal rate at steady state (Fig. 3). Furthermore, we found that Cel6A has a very high rate of the inner processive cycle, which comprises the chemical reactions and one processive step forward. While a precise rate constant for this inner cycle could not be measured with the time resolution at hand, we estimated the value to be at least 20 s^{-1}, which is among the highest turnovers reported for cellulases. This rapid turnover of the inner cycle suggests that slow enzymatic breakdown of cellulose is not a question of a particularly high energy barrier for hydrolysis of the β-1,4 bond, but rather a result of other, non-covalent factors including low accessibility and slow dissociation from the substrate surface. Finally, we found that the on/off dynamics of Cel6A is at least an order of

magnitude faster than for the other CBH from *T. reesei*, Cel7A. This rapid on/off dynamic of Cel6A may be a functional advantage, but it appears to come at a penalty of lower ability of attacking broad range of sites on the cellulose surface. Thus, we found that the density of attack sites for Cel6A was much lower than the density of adsorption sites, and we suggest that this reflects an inability to attack a broad range of structurally distinct sites on the cellulose surface. When comparing the overall efficacy of Cel6A and Cel7A this high physical specificity (or selectivity) was the major limitation of Cel6A.

Materials and methods

Enzyme

Cel6A from *T. reesei* was heterologously expressed in *Aspergillus oryzae* and purified as described elsewhere [38, 39], to obtain one single band on a sodium dodecyl sulfate polyacrylamide gel. The enzyme concentration was determined by absorbance at 280 nm using a theoretical extinction coefficient [40] of 97,790 $M^{-1}cm^{-1}$.

Substrates

All experiments were performed in a standard buffer consisting of 50 mM sodium acetate, pH 5.0. Avicel (PH101, Sigma Aldrich 11365) was washed three times in water and two times in standard buffer to remove traces of soluble sugars and subsequently prepared by dispersion for 20 min by using an ultra Turrax T25 Basic (IKA, Staufen, Germany) coaxial homogenizer. This latter procedure produces a quite uniform suspension of smaller particles, which is essential for passage through the tubes in the quenched-flow apparatus [16]. RAC was prepared from Avicel as described elsewhere [41] with following modifications. After suspending the Avicel in MQ water 8 mL of ice-cold 85 % orthophosphoric acid was added. Centrifugation was done at 2500 g for 20 min. The substrate was resuspended in standard buffer and pH was adjusted to 5.0 with 10% HCl. The final concentration of the substrate was determined by dry matter weight measurements.

Progress curves

We used a recently developed quenched-flow apparatus suited for reactions with enzymes acting on solid substrates [16]. In brief, the method relies on a peristaltic pump that generates a constant flow. The enzyme and substrate are mixed in a mixing tee and subsequently “aged” in loops of different length. The reaction is quenched by mixing with NaOH to a final concentration of 0.1 M in a subsequent mixing tee. The time resolution was varied by changing between loops of different lengths and different flow rates [16]. Reactions consisted of 0.2 µM Cel6A and 8 g/L Turraxed Avicel or 1.8 g/L RAC. Blanks were created in which the enzyme was quenched with NaOH prior to mixing with the substrate in quenched-flow apparatus. The reaction time used in the quenched-flow apparatus ranged from 0.25-5.7 s. All experiments were performed at 20°C. Product concentrations were determined by High-Performance Anion-Exchange Chromatography with Pulsed Amperometric Detection (HPAEC-PAD) using a Dionex ICS-5000 instrument fitted with a CarboPac PA10 column (Thermo Scientific, Waltham, MA). Concentrations were calculated against an external standard

containing known concentrations of glucose, cellobiose and cellotriose. Non-linear regression analysis of the quench flow data relies on a simplified description of processive hydrolysis (Scheme 1) and an analytical solution for the time dependent concentration of cellobiose, *C(t)*, derived by Praestgaard, et al. [14] .

Steady state kinetics

We measured the steady state kinetics under conditions where either the enzyme concentration or the substrate load were varied systematically. In one trial, we used a fixed enzyme concentration of 0.2 µM and 11 different loads of substrate between 0.9 and 42 g/L (Turraxed Avicel) or 0.2 to 5 g/L (RAC). We made triplicate measurements for each substrate load. In another trial, we used a fixed substrate load of either 2 g/L (Turraxed Avicel) or 0.5 g/L (RAC) and ten different enzyme concentration ranged from 0.05 – 8 µM. Hydrolysis was done for 1 h at 20°C shaking at 1100 rpm followed by quenching by centrifugation at 2500 g for 3 min. Reducing sugar end concentrations in the supernatant were quantified by the *para*-hydroxybenzoic acid hydrazide (PAHBAH) method [42]. The experimental procedures of the assay is described in [39]. Absorption at 405 nm was determined by using a plate reader (Spectra Max 3, Molecular Devices, Sunnyvale, Ca) and compared to a cellobiose standard series with concentrations from 0-1000 µM. All steady state rates were determined by taking the slope of the cellobiose concentration from t = 0-1h. Non-linear fits to Eqn (1), Eqn (2) was made by using the software Origin pro 2017 (OriginLab Coorporation, Northampton, MA 01060, USA).

Binding isotherms

To assess binding we prepared samples with fixed loads of either Turraxed Avicel (10 g/L) or RAC (2 g/L) and 10 different concentrations of Cel6A between 0.019 µM and 6 µM. Samples were incubated for 1 h at 20°C followed by centrifugation at 2500 g for 3 min. 50 µL of the supernatant was diluted in 150 µL standard buffer and enzyme concentrations were determined by the intrinsic fluorescence as described elsewhere [39]. Concentrations were calculated against standards containing the same enzyme initial concentrations in standard buffer.

Product profile

Reactions consisting of 8 g/L Turraxed Avicel or 1.8 g/L RAC and 0.2 µM Cel6A were manually quenched after 5-30 s by mixing with NaOH to a final concentration of 0.1 M. The concentration of glucose, cellobiose and cellotriose was determined by HPAEC-PAD as described above. The product ratio was calculated as % of the total amount of sugars. This ratio was nearly constant at all applied reaction times (5, 10, 20 and 30 s).

Acknowledgements

This work was supported by the Innovation Fund Denmark [grant number 5150-00020B] and the Novo Nordisk Foundation [Grant number NNF15OC0016606].

Author contributions

SJC, JK, SFB, KB and PW conceived and designed the study. SJC purified enzymes, planned and carried out the experiments, and analyzed the data. JK carried out mathematical modeling of the quenched-flow data. KB provided the enzymes used in the study. SJC and PW wrote the manuscript with support from SFB and JK. All authors reviewed and approved the manuscript.

References

1. Teeri TT (1997) Crystalline cellulose degradation: New insight into the function of cellobiohydrolases, *Trends Biotechnol.* **15**, 160-167.
2. Nidetzky B & Claeyssens M (1994) Specific quantification of trichoderma reesei cellulases in reconstituted mixtures and its application to cellulase-cellulose binding studies, *Biotechnol Bioeng.* **44**, 961-6.
3. Rosgaard L, Pedersen S, Langston J, Akerhielm D, Cherry JR & Meyer AS (2007) Evaluation of minimal Trichoderma reesei cellulase mixtures on differently pretreated Barley straw substrates, *Biotechnol Prog.* **23**, 1270-6.
4. Davies G & Henrissat B (1995) Structures and mechanisms of glycosyl hydrolases, *Structure.* **3**, 853-9.
5. Divne C, Stahlberg J, Reinikainen T, Ruohonen L, Pettersson G, Knowles JK, Teeri TT & Jones TA (1994) The three-dimensional crystal structure of the catalytic core of cellobiohydrolase I from Trichoderma reesei, *Science.* **265**, 524-8.
6. Rouvinen J, Bergfors T, Teeri T, Knowles JK & Jones TA (1990) Three-dimensional structure of cellobiohydrolase II from Trichoderma reesei, *Science.* **249**, 380-6.
7. Payne CM, Knott BC, Mayes HB, Hansson H, Himmel ME, Sandgren M, Stahlberg J & Beckham GT (2015) Fungal cellulases, *Chem Rev.* **115**, 1308-448.
8. Harjunpaa V, Teleman A, Koivula A, Ruohonen L, Teeri TT, Teleman O & Drakenberg T (1996) Cello-oligosaccharide hydrolysis by cellobiohydrolase II from Trichoderma reesei. Association and rate constants derived from an analysis of progress curves, *Eur J Biochem.* **240**, 584-91.
9. Koivula A, Ruohonen L, Wohlfahrt G, Reinikainen T, Teeri TT, Piens K, Claeyssens M, Weber M, Vasella A, Becker D, Sinnott ML, Zou JY, Kleywegt GJ, Szardenings M, Stahlberg J & Jones TA (2002) The active site of cellobiohydrolase Cel6A from Trichoderma reesei: the roles of aspartic acids D221 and D175, *J Am Chem Soc.* **124**, 10015-24.
10. Nakamura A, Tasaki T, Ishiwata D, Yamamoto M, Okuni Y, Visootsat A, Maximilien M, Noji H, Uchiyama T, Samejima M, Igarashi K & Iino R (2016) Single-molecule Imaging Analysis of Binding, Processive Movement, and Dissociation of Cellobiohydrolase Trichoderma reesei Cel6A and Its Domains on Crystalline Cellulose, *J Biol Chem.* **291**, 22404-22413.
11. Nidetzky B, Zachariae W, Gercken G, Hayn M & Steiner W (1994) Hydrolysis of cellooligosaccharides by Trichoderma reesei cellobiohydrolases: Experimental data and kinetic modeling, *Enzyme and microbial technology.* **16**, 43-52.

12. Badino SF, Kari J, Christensen SJ, Borch K & Westh P (2017) Direct kinetic comparison of the two cellobiohydrolases Cel6A and Cel7A from Hypocrea jecorina, *Biochimica et Biophysica Acta (BBA)-Proteins and Proteomics.* **1865**, 1739-1745.
13. Claeyssens M, Tomme P, Brewer CF & Hehre EJ (1990) Stereochemical course of hydrolysis and hydration reactions catalysed by cellobiohydrolases I and II from Trichoderma reesei, *FEBS Lett.* **263**, 89-92.
14. Praestgaard E, Elmerdahl J, Murphy L, Nymand S, McFarland KC, Borch K & Westh P (2011) A kinetic model for the burst phase of processive cellulases, *FEBS J.* **278**, 1547-60.
15. Jalak J & Väljamäe P (2010) Mechanism of initial rapid rate retardation in cellobiohydrolase catalyzed cellulose hydrolysis, *Biotechnology and bioengineering.* **106**, 871-883.
16. Olsen JP, Kari J, Borch K & Westh P (2017) A quenched-flow system for measuring heterogeneous enzyme kinetics with sub-second time resolution, *Enzyme Microb Technol.* **105**, 45-50.
17. Cruys-Bagger N, Elmerdahl J, Praestgaard E, Borch K & Westh P (2013) A steady-state theory for processive cellulases, *FEBS J.* **280**, 3952-61.
18. Kari J, Andersen M, Borch K & Westh P (2017) An Inverse Michaelis-Menten Approach for Interfacial Enzyme Kinetics, *Acs Catal.* **7**, 4904-4914.
19. Andersen M, Kari J, Borch K & Westh P (2018) Michaelis-Menten equation for degradation of insoluble substrate, *Math Biosci.* **296**, 93-97.
20. Jalak J & Väljamäe P (2014) Multi-mode binding of cellobiohydrolase Cel7A from Trichoderma reesei to cellulose, *PloS one.* **9**, e108181.
21. Horn SJ, Sorlie M, Varum KM, Valjamae P & Eijsink VG (2012) Measuring processivity, *Methods in enzymology.* **510**, 69-95.
22. Vuong TV & Wilson DB (2009) Processivity, synergism, and substrate specificity of Thermobifida fusca Cel6B, *Applied and environmental microbiology.* **75**, 6655-6661.
23. Velleste R, Teugjas H & Väljamäe P (2010) Reducing end-specific fluorescence labeled celluloses for cellulase mode of action, *Cellulose.* **17**, 125-138.
24. Gruno M, Valjamae P, Pettersson G & Johansson G (2004) Inhibition of the Trichoderma reesei cellulases by cellobiose is strongly dependent on the nature of the substrate, *Biotechnol Bioeng.* **86**, 503-11.
25. Gutfreund H & Sturtevant JM (1956) Mechanism of the Reaction of Chymotrypsin with Para-Nitrophenyl Acetate, *Biochemical Journal.* **63**, 656-661.
26. Hartley BS & Kilby BA (1954) The reaction of p-nitrophenyl esters with chymotrypsin and insulin, *Biochemical Journal.* **56**, 288-297.
27. Fersht A (1998) *Structure and Mechanism in Protein Science*, 2nd edn, W.H. Freeman and Company, New York.
28. Segel IH (1975) *Enzyme kinetics: behavior and analysis og rapid equilibrium and steady-state enzyme systems*, John Wiley & Sons Inc., New York.
29. Lucius AL, Maluf NK, Fischer CJ & Lohman TM (2003) General methods for analysis of sequential "n-step'' kinetic mechanisms: Application to single turnover kinetics of helicase-catalyzed DNA unwinding, *Biophysical Journal.* **85**, 2224-2239.
30. Igarashi K, Uchihashi T, Uchiyama T, Sugimoto H, Wada M, Suzuki K, Sakuda S, Ando T, Watanabe T & Samejima M (2014) Two-way traffic of glycoside hydrolase family 18 processive chitinases on crystalline chitin, *Nature communications.* **5**, 3975.
31. Kuusk S, Sorlie M & Valjamae P (2015) The predominant molecular state of bound enzyme determines the strength and type of product inhibition in the hydrolysis of recalcitrant polysaccharides by processive enzymes, *J Biol Chem.* **290**, 11678-91.
32. Koivula A, Kinnari T, Harjunpää V, Ruohonen L, Teleman A, Drakenberg T, Rouvinen J, Jones TA & Teeri TT (1998) Tryptophan 272: an essential determinant of crystalline cellulose degradation by Trichoderma reesei cellobiohydrolase Cel6A, *FEBS Letters.* **429**, 341-346.

33. Karuna N & Jeoh T (2017) The productive cellulase binding capacity of cellulosic substrates, *Biotechnology and Bioengineering.* **114**, 533-542.
34. Cruys-Bagger N, Elmerdahl J, Praestgaard E, Tatsumi H, Spodsberg N, Borch K & Westh P (2012) Pre-steady-state kinetics for hydrolysis of insoluble cellulose by cellobiohydrolase Cel7A, *Journal of Biological Chemistry.* **287**, 18451-18458.
35. Cruys-Bagger N, Tatsumi H, Ren GR, Borch K & Westh P (2013) Transient kinetics and rate-limiting steps for the processive cellobiohydrolase Cel7A: effects of substrate structure and carbohydrate binding domain, *Biochemistry.* **52**, 8938-8948.
36. Varrot A, Frandsen TP, von Ossowski I, Boyer V, Cottaz S, Driguez H, Schülein M & Davies GJ (2003) Structural basis for ligand binding and processivity in cellobiohydrolase Cel6A from Humicola insolens, *Structure.* **11**, 855-864.
37. Zou J-y, Kleywegt GJ, Ståhlberg J, Driguez H, Nerinckx W, Claeyssens M, Koivula A, Teeri TT & Jones TA (1999) Crystallographic evidence for substrate ring distortion and protein conformational changes during catalysis in cellobiohydrolase Ce16A from Trichoderma reesei, *Structure.* **7**, 1035-1045.
38. Borch K, Jensen K, Krogh K, Mcbrayer B, Westh P, kari J, Olsen J, Sørensen T, windahl M & Xu H (2014) Cellobiohydrolase variants and polynucleotides encoding same in, WO2014138672 A1
39. Sørensen TH, Cruys-Bagger N, Windahl MS, Badino SF, Borch K & Westh P (2015) Temperature effects on kinetic parameters and substrate affinity of Cel7A cellobiohydrolases, *Journal of Biological Chemistry.* **290**, 22193-22202.
40. Gasteiger E, Hoogland C, Gattiker A, Duvaud Se, Wilkins MR, Appel RD & Bairoch A (2005) Protein Identification and Analysis Tools on the ExPASy Server in *The Proteomics Protocols Handbook* (Walker, J. M., ed) pp. 571-607, Humana Press, Totowa, NJ.
41. Zhang Y-HP, Cui J, Lynd LR & Kuang LR (2006) A transition from cellulose swelling to cellulose dissolution by o-phosphoric acid: evidence from enzymatic hydrolysis and supramolecular structure, *Biomacromolecules.* **7**, 644-648.
42. Lever M (1973) Colorimetric and fluorometric carbohydrate determination with p-hydroxybenzoic acid hydrazide, *Biochemical medicine.* **7**, 274-281.

Table 1. Kinetic parameters [a] for *Tr*Cel6A hydrolysis of RAC and Avicel derived from non-linear regression analysis of the pre-steady state data in Fig. 1

Substrate	Parameters		
	k_{on} ((g/L)$^{-1}$s^{-1})	k_{off} (s^{-1})	*n*
Avicel	0.29±0.19	0.32±0.06	7.6±0.9
RAC	0.93±0.24	0.33±0.04	12.1±1.1

[a]Standard errors are from the non-linear regression of the model to the experimental data.

Table 2. Steady state kinetic parameters[a] for *Tr*Cel6A hydrolysis of Avicel and RAC derived from Fig. 2

Substrate	Steady state parameters					
	^{conv}MM		^{inv}MM		Adsorption	
	$^{conv}V_{max}/E_0$ (s^{-1})	$^{conv}K_M$ (g/L)	$^{inv}V_{max}/S_0$ (µmol g^{-1}s^{-1})	$^{inv}K_M$(µM)	Γ_{max} (µmol/g)	Γ_{attack} (µmol/g)[b]
Avicel	0.41±0.02	9.56±1.08	0.0241±0.0003	0.34±0.02	0.37±0.08	0.059±0.003[a]
RAC	0.65±0.03	3.64±0.24	0.0865±0.0037	0.44±0.08	3.57±0.10	0.133±0.008[a]

[a]Standard errors are from the non-linear regression of Eqn (1), (2) and (3) to the experimental data. [b]Γ_{attack} was derived from Eqn (4) as described in the main text.

Table 3. Average product ratios in % of total sugar for *Tr*Cel6A hydrolysis of RAC and Avicel

Substrate	Product ratio (%)[c]			Processivity
	G1[a]	**G2**[a]	**G3**[a]	n^{prod}
Avicel	nd	83.2 ± 0.8	16.8 ± 0.8	5.0 ± 0.29[b]
RAC	4.4 ± 0.3	85.5 ± 0.4	10.1 ± 0.2	5.6 ± 0.19[b]

[a]G1-3 reflects glucose, cellobiose and cellotriose. [b]The processivity numbers estimated from the ratio ([G2]-[G1])/([G3]+[G1]) suggested earlier [22]. [c]Errors represent ±SD of experimental data points.

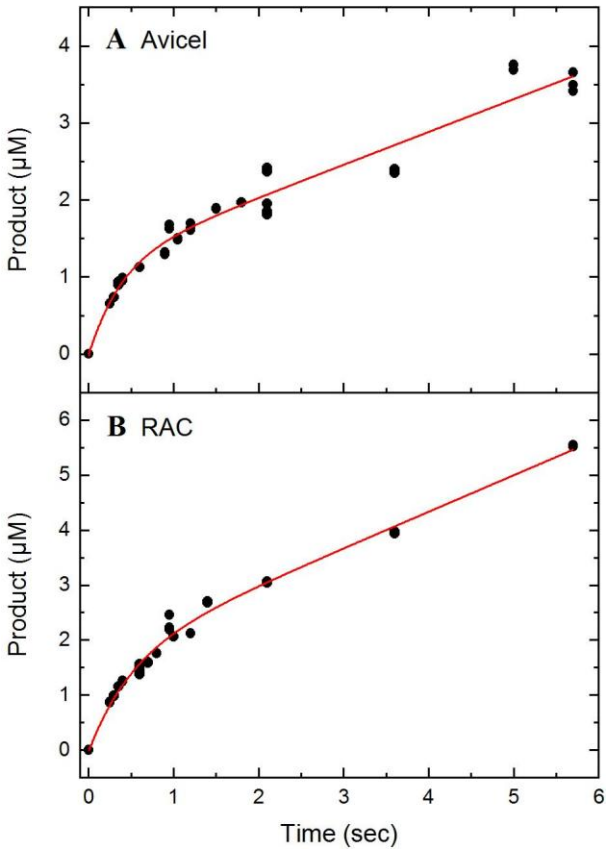

Fig. 1 Progress curves from quenched-flow experiments for TrCel6A. Product concentration reflects the sum of the cellobiose- and cellotriose concentration. The enzyme concentration was 0.2 µM and the substrate load was 8 g/L Avicel (Panel A) or 1.8 g/L RAC (Panel B). Experiments were performed at 20°C, pH 5. Circles represent experimental data points and red lines are the best non-linear regression fit to the model in Scheme 1.

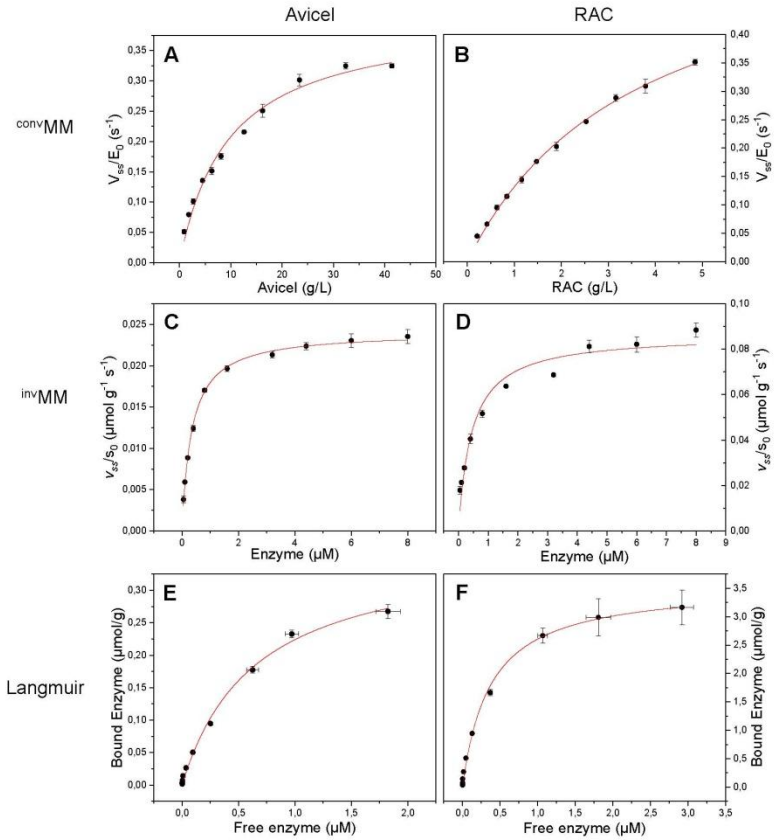

Fig. 2 Three types of saturation behavior of TrCel6A on respectively Avicel (left column) and RAC (right column). Top row (A+B) shows conventional Michaelis-Menten data (constant, low enzyme concentration and variable substrate loads). Symbols represents experimental data and red lines are best first of Eqn (1). 0.2 µM Cel6A was used. Middle row, (C+D), shows data from inverse Michaelis-Menten analysis (constant, low substrate load and variable enzyme concentration) with best fits of Eqn (2). 2.0 and 0.5 g/L Avicel and RAC was used, respectively. The lower row (E+F) shows binding isotherms (bound enzyme vs. free enzyme) with best fits of Eqn (3). 10 and 2.5 g/L Avicel and RAC was used, respectively. Error bars represent ±SD of triplicate experiments. All experiments were performed at 20°C, pH 5.

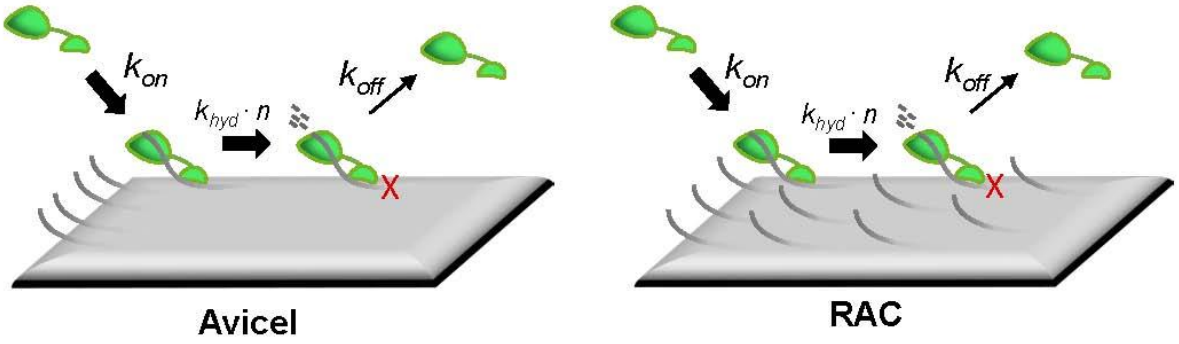

Fig. 3 Illustration of the processive breakdown of cellulose by Cel6A on two different cellulosic substrates, microcrystalline Avicel and amorphous RAC. Our description of the reaction comprises three reactions steps: adsorption to the cellulose surface (governed by k_{on}), hydrolytic reaction and processive movement ($k_{hyd} \cdot n$) and dissociation from the surface (k_{off}). The width of the arrows reflects approximate rates of each reaction step. After n catalytic steps, the enzyme encounters a steric obstacle (red cross). Since dissociation is slow on both substrates, unproductive Cel6A accumulates on the cellulose surface. RAC contains ~2.3 times more attack sites (gray threads) on which Cel6A can initiate hydrolysis (Γ_{attack}) compared to Avicel. This difference is the main reason for higher catalytic rate on RAC.

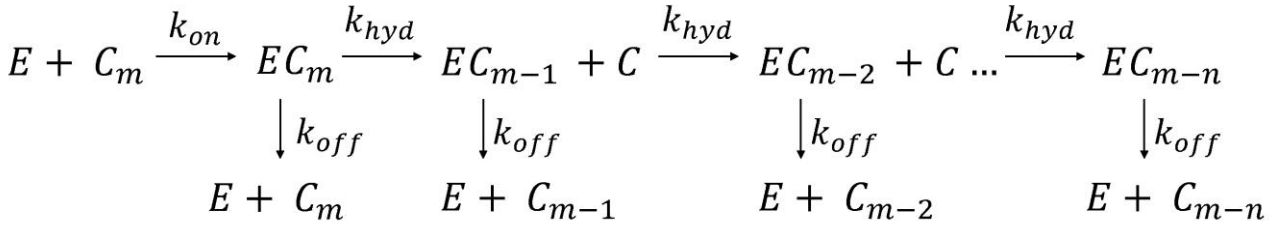

Scheme 1. Simplified reaction mechanisms for the processive breakdown of cellulose by Cel6A. One cellulose strand with m cellobiose moieties (C_m) is attacked by the enzyme (E) and gradually shortened (C_{m-1}, C_{m-2} etc.) as cellobiose (C) is released. Kinetic equations for this scheme have been described elsewhere [14]